Virtual Screening of Curcumin and its Analogs against the Spike Surface Glycoprotein of SARS-CoV-2 and SARS-CoV

Ashish Patel[1], Malathi Rajendran[2], Ashish Shah[3], Harnisha Patel[4], Suresh B. Pakala[5] Prashanthi Karyala[2#]

[1] Ramanbhai Patel College of Pharmacy, Charotar University of Science and Technology, Changa-388421, Gujarat, India

[2] Department of Biochemistry, Indian Academy Degree College - Autonomous, Hennur Main Road, Bengaluru-560043, Karnataka, India

[3] Department of Pharmacy, Sumandeep Vidyapeeth , Vadodara-391760, Gujarat, India

[4] Parul Institute of Pharmacy, Parul University, Vadodara-391760, Gujarat, India

[5] Biology Division, Indian Institute of Science Education and Research (IISER) Tirupati, Karakambadi Road, Mangalam, Tirupati-517507, Andhra Pradesh, India

[#] **Corresponding Author**

Dr. Karyala Prashanthi

Department of Biochemistry

Indian Academy Degree College – Autonomous

Hennur Main Road, Bengaluru – 560043

Karnataka, India

e-mail: prashanthi@indianacademy.edu.in

Phone: 91-80-67458937

Fax: 91-80-67458908

Abstract

COVID-19, a new pandemic caused by SARS-CoV-2, was first identified in 2019 in Wuhan, China. The novel corona virus SARS-CoV-2 and the 2002 SARS-CoV have 74 % identity and use similar mechanisms to gain entry into the cell. Both the viruses enter the host cell by binding of the viral spike glycoprotein to the host receptor, angiotensin converting enzyme 2 (ACE2). Targeting entry of the virus has a better advantage than inhibiting the later stages of the viral life cycle. The crystal structure of the SARS-CoV (6CRV: full length S protein) and SARS-CoV-2 Spike proteins (6M0J: Receptor binding domain, RBD) was used to determine potential small molecule inhibitors. Curcumin, a naturally occurring phytochemical in *Curcuma longa,* is known to have broad pharmacological properties. In the present study, curcumin and its derivatives were docked, using Autodock 4.2, onto the 6CRV and 6M0J to study their capability to act as inhibitors of the spike protein and thereby, viral entry. The curcumin and its derivatives displayed binding energies, ΔG, ranging from -14.18 to -4.04 kcal/mol (6CRV) and -10.01 to -5.33 kcal/mol (6M0J). The least binding energy was seen in bis-desmethoxycurcumin with: ΔG = -14.18 kcal/mol (6CRV) and -10.01 kcal/mol (6M0J). A good binding energy, drug likeness and efficient pharmacokinetic parameters suggest the potential of curcumin and few of its derivatives as SARS-CoV-2 spike protein inhibitors. However, further research is necessary to investigate the ability of these compounds as viral entry inhibitors.

Key words: Curcumin, SARS-CoV-2, SARS-CoV, spike protein

Introduction:

Coronaviruses are enveloped positive-sense single stranded RNA viruses that belong to the family coronaviridae. They usually infect birds and mammals and cause mild respiratory diseases (Kahn & McIntosh 2005). However, in the recent past, these viruses have caused lethal endemics such as Severe Acute Respiratory Syndrome (SARS) and Middle East Respiratory Syndrome (MERS) endemics (Kahn & McIntosh 2005). In December 2019, Wuhan city in China became the centre of a surge in cases of pneumonia by an unknown cause (Gorbalenya 2020). A novel corona virus, called SARS-CoV-2, was isolated from these pneumonia patients in January 2020 (Gorbalenya 2020) and the disease was called the **Co**rona**vi**rus **d**isease 20**19** (COVID-19) by the World Health Organization in February, 2020 (Jiang et al. 2020; Who 2020). Even though the epidemic may have started from a zoonotic transmission in a seafood market, that also sold wild animals, it became clear that this disease was transmitted from person to person (Li et al. 2020). The clinical characteristics of this disease are broad, constituting asymptomatic infections, mild respiratory disease, severe pneumonia with respiratory failure and even death (Chen et al. 2020; Huang et al. 2020; Wang et al. 2020). The COVID-19 pandemic poses a significant challenge to global public health (Phelan, Katz & Gostin 2020), appealing for the development of safe and successful prophylactics and therapies against infection of its causative agent, the SARS-CoV-2 virus.

SARS-CoV-2 has a genome of ~30 kilobases, which codes for multiple structural and non-structural proteins (Kahn & McIntosh 2005). The structural proteins, present on the surface of the mature virion, include the spike protein, the membrane protein, the envelope protein and the nucleocapsid protein (Kahn & McIntosh 2005). The Spike protein, of the betacorona viruses SARS-CoV-2 and SARS-CoV, enables the attachment of the virus to the cells of the lower respiratory tract of humans to gain entry into the lung tissue (Hoffmann et al. 2020). Apart from attachment, the spike glycoprotein also appears to play a role in fusion and entry of the virus into the host (Chen, Guo, Pan & Zhao 2020; Hoffmann et al. 2020). The spike protein, of the novel coronavirus, utilizes the SARS-CoV receptor, ACE2 for entry (Chen et al. 2020) and the spike protein is primed by the cellular protease, TMPRSS2 (Hoffmann et al. 2020). A serine protease inhibitor, which can act on TMPRSS2, has been shown to inhibit novel coronavirus entry (Hoffmann et al. 2020). Therefore, the spike protein of the novel coronavirus is a good drug

target and identifying small molecules that bind to S protein would inhibit viral recognition of host cells and disrupt viral-host interactions.

Curcumin, a naturally occurring phytochemical and principal component of Curcuma longa, has exhibited broad pharmacological properties including antioxidant, anti-inflammatory, anti-cancer and anti-viral effects (Kocaadam & Åžanlier 1080; Lal, Gupta, Thavaselvam & Agarwal 2016; Wiggers et al. 2017; Khor, Aluwi, Rullah & Lam 2019). Curcumin and its derivatives, due to its rich conventional medicinal interest, has undergone comprehensive *in vitro* and *in vivo* studies. It has, therefore, been associated with more than 100 cellular targets, including cytokine s, proteins, transcription factors, and receptors. Previous studies have shown the potential of curcumin as a treatment against Influenza A virus infection, by an effect mediated by modulating immune response to prevent injury to the lung tissue (Han, Xu, Guo & Huang 2018). Curcumin has also been shown to have anti neuraminidase (NA) activity for the influenza virus NA protein (Richart et al. 2018). Therefore, in the present study, curcumin and its derivatives were docked onto the spike protein of the SARS-CoV and the SARS-CoV-2 to predict the binding interactions.

We found that curcumin and few of its derivatives showed promising results to be potential spike protein inhibitors. One of the derivatives, **bis demethoxy curcumin**, showed the best binding affinity to the spike protein of both the SARS-CoV and the novel corona virus, SARS-CoV-2. The possibility for few of the curcumin derivatives, that showed good binding affinity, could be tested for further therapeutic use against COVID-19.

Experimental Section

Sequence Analysis

The sequences of the SARS-CoV-2 and SARS-CoV were downloaded from National Center for Biotechnology Information. Multiple sequence analysis and pairwise sequence identity was determined using the Clustal Omega server at the European Bioinformatics Institute (Sievers et al. 2011).

Preparation of coordinate file

The X-ray crystal structure of spike surface glycoprotein of SARS-CoV (PDB entry: 6CRV, resolution = 3.2 Å) and co-crystallized structure of SARS-CoV-2 RBD with human ACE2 Protein (PDB entry: 6M0J, resolution = 2.45 Å) was retrieved from Protein Data Bank (https:/www.rscb.org/pdb). The protein structure was prepared using the Discovery Studio Visualizer (version 3.1) and AutoDock Tools (ADT; version 1.5.4) through different steps viz. removal of water molecules and co-crystallized ligand, addition of missing hydrogen atoms, addition of Gasteiger-Marsili and Kollman charges, merging of non-polar hydrogens, and assignment of rotatable bonds. The file was then saved in pdbqt file format for further analysis.

Preparation of ligands

The chemical structures of curcumin derivatives were constructed using Chem3D 15.0 module of ChemOffice 15.0 and saved in PDB format. The structures were optimized using "Prepare Ligands" in the AutoDock 4.2, flexible torsions were assigned and the acyclic dihedral angles were allowed to rotate freely. The file was then saved as pdbqt file format for further analysis.

Molecular Docking

Molecular docking simulations were conducted on the curcumin derivatives using the AutoDock 4.2 to get insight into their binding preferences within the active site of the receptor. The molecular docking simulations were performed on the PC based machines running on Windows 7 (x86) as operating system. The software included MGL tools 1.5.4 based AutoDock 4.2 (www.scripps.edu) which uses Python 2.7 language - Cygwin C:\ program (www.cygwin.com) and Python 2.5 (www.python.com) (Morris et al. 2009). The docked molecules within the active site were visualized using Discovery Studio Visualizer 3.1 (2012).

Docking Methodology

The flexible docking was performed using the refined spike protein of SARS-CoV (6CRV) and RBD domain of SARS-CoV-2 (6MOJ). The grid maps of the interaction energies of various atom types were pre-calculated using AutoGrid 4.2. In each docking for spike surface glycoprotein and spike RBD, a grid box was created using a grid map of 45×45×45 points,

60×60×60 points with grid spacing of 0.375 Å and 0.420 Å respectively. The grid maps were centred on the corresponding ligand binding site within the protein structure.

Lamarckian Genetic Algorithm (LGA) was adopted to perform docking simulations using the following default parameters, viz. 100 independent runs with step sizes of 0.2 Å for translations and 5 Å for orientations and torsions, an initial population of random individuals with a population size of 150 individuals, a maximum of 2.5 x 106 energy evaluations, maximum number of generations of 27,000; mutation and crossover rates of 0.02 and 0.8 respectively and an elitism value of 1. All the computations were carried out on Cygwin and was used to generate both grid parameter file (.gpf file) and docking parameter file (.dpf file) for each ligand. The docked conformations of each ligand were ranked into clusters based on the binding energy and the top ranked conformations were used for further study. The pose with the lowest ΔG-score was considered the best fitted one and was further analyzed for Ligand-receptor interactions.

In-silico drug-likeness and pharmacokinetic property prediction

The in-silico prediction studies were performed, using pkCSM online prediction platforms (Pires, Blundell & Ascher 2015), to assess the theoretical pharmacokinetic parameters of the ligands to predict the drug-likeness of ligands. The software calculated pharmaceutically relevant properties such as H-bond donor, H-bond acceptor, octanol-water partition coefficient (LogP), surface area, and number of rotatable bonds. in addition to the effect of ligands on ADME parameters like water solubility, Caco2 permeability, human intestinal absorption, skin permeability, P-glycoprotein I and II inhibition, volume of distribution, fraction of unbound drug, Blood Brain Barrier and CNS permeability, cytochrome P450 (CYP3A4 and CYP2C9 inhibition) inhibition, total clearance, action as renal OCT2 (organic cation transporter 2) substrate.

Results

Sequence alignment of the SARS-CoV-2 and SARS-CoV Spike protein sequences

Prior to performing the docking studies the multiple sequence alignment was carried out for the spike proteins of the novel corona virus, SARS-CoV-2 and the 2002 SARS-CoV (**Figure 1**). These results show that there is a very high percentage identity (greater than 99 %) among the spike protein of the novel corona viruses. There was around 74 % identity of the novel corona

virus spike proteins with the 2002 SARS-CoV. Therefore, the SARS-CoV-2 spike protein is very much closer to SARS-CoV than to the other corona viruses as shown in other studies (Ahmed, Quadeer & McKay 2020).

Molecular Docking Studies

The three dimensional structure of the SARS-CoV and SARS-CoV-2 RBD has been solved. The PDB files of the SARS-CoV spike protein (6CRV) and the receptor binding domain of the SARS-CoV-2 (6M0J) was downloaded from the PDB databank. These structures were used to predict the ability of the binding of curcumin and its derivatives to the spike proteins of the two corona viruses. Curcumin and 24 of its derivatives **(Figure 2 and Supplementary figure 1**) were docked on to SARS-CoV Spike surface Glycoprotein (6CRV) and of SARS-CoV-2 Spike RBD (6MOJ). **Table 1** and **2** gives the binding energies of curcumin and its derivatives with 6CRV (binding energies ranged from -14.18 to -4.04 kcal/mol) and with 6MOJ (binding energies ranged -10.01 to -5.33 kcal/mol). Visual examination of the computationally docked optimal binding poses of curcumin and its derivatives on the spike surface glycoprotein and spike RBD revealed the important role of various types of interactions viz. hydrogen bonding and hydrophobic interactions, including $\pi - \pi$ stacking, π – cation, and $\pi - \sigma$ interactions in the stability of curcumin/deriavatives - 6CRV / 6MOJ. All compounds showed one or more hydrogen bonds with 6CRV and 6MOJ except a few.

In 6CRV, it was found that CYS 145, HIS 164, PHE 140, LEU 141, GLN 189, MET 165, GLU 166, SER144, GLY143 were the major amino acids involved in hydrogen bonding and hydrophobic interaction with most of the curcumin compounds. However, majority of the curcumin compounds exhibit hydrogen bonding with SER 144, LEU 141, GLU 166 and HIS 164 except compound 1 and 9. In addition, all the compounds exhibited hydrophobic ($\pi - \pi$ stacking, π – cation, and $\pi - \sigma$) interactions with PHE 140, GLN 189, GLU 166, CYS 145, MET 159, GLY 143.

All compounds showed one or more hydrogen bonding interactions with spike RBD of the SARS-CoV-2 (6M0J) except 3-5-di-tert-butyl-4-hydroxybenzaldehyde curcumin. It was found that ARG355, TYR396, PRO426, ASP428, THR430, GLY431, PHE429, PHE 464, GLU 516, SER 514, LEU 517 and PHE 515 were the major amino acids involved in hydrogen bonding and

hydrophobic interaction with the all of curcumin compounds. However, majority of the curcumin compounds exhibit hydrogen bonding with ARG 355, LEU 517 and THR 430. In addition, the compounds exhibited hydrophobic (π – π stacking, π – cation, and π – σ) interactions with PHE 464, GLY 431, GLU 516, SER514, PHE 515, TYR 396, PRO 426, ASP 428 and PHE 429 respectively.

The curcumin derivative with the best binding affinity was **Bis demethoxy curcumin** for both 6CRV (ΔG = -14.18 kcal/mol) and 6MOJ (ΔG = -10.01 kcal/mol). The native compound, curcumin, demonstrated a binding energy of -9.81 kcal/mol for 6MOJ and -10.2 kcal/mol for 6CRV. Binding mode of **Bis demethoxy curcumin** with SARS-CoV Spike protein and SARS-CoV-2 Spike protein RBD is shown in **Figure 3** and **4** respectively.

In-silico drug-likeness and pharmacokinetic property prediction

All the structures used for docking were analysed for *in silico* drug-likeness based on the Lipinski's rules using pkCSM server (**Table 3**). The lipophilicity (expressed as LogP) predicted for all the compounds were found to be well above the traditionally cut-off value of 5 used for drug design. Curcumin and its derivatives, used in this study, show suitable MW values (MW < 500) essential for a successful penetration through biological membranes. The surface area (SA) for all the compounds was observed to be in the range 115.89 - 240.65 $Å^2$ which is well within the limit. All compounds, except **5-di-tert-butyl-4-hydroxybenzaldehyde curcumin (BHBC), 4-methoxy-1-naphthaldehyde curcumin (MNC), Syringaldehyde curcumin (SYC) and compound-16,** fall into the appropriate range indicating good bioavailability of the candidate molecule. The number of hydrogen bond acceptors (HBA, ≤10) and donors (HBD, ≤5) for all the compounds were in accordance with the Lipinski's rule of five.

Additionally, a variety of key ADMET (Absorption, Distribution, Metabolism and Excretion) properties have also been calculated with the aid of pkCSM server. The results are listed in **Table 4**. All curcumin derivatives showed moderate to high water solubility ranging from -2.91 log mol/L (**BHBC**) to -6.99 log mol/L (**compound-12**), in addition to high Caco-2 permeability (permeation > 0.90) except compound **BHBC and MNC** (permeation = 0.67 and 0.43 respectively) which showed moderate permeability. Intestinal absorption (IA) has been found to be greater than 85% indicating good permeation across the intestinal membrane. Further, all curcumin compounds showed good permeation through skin (permeation > -2.5). Additionally,

all curcumin compounds showed no inhibition towards P-glycoprotein I and P-glycoprotein II, except compounds **BHBC, MNC, compound-13** and Ferrulic acid curcumin (**FAC)** which demonstrated inhibition towards P-glycoprotein I. Furthermore, all curcumin compounds showed poor BBB permeability and moderate CNS permeability except **Isovanillin curcumin (IVC), SYC**. All showed inhibition towards the metabolizing enzyme CYP3A4 except **BHBC, compounds-8, -11, -14, -15 and -16**, while except compound-**15** all showed inhibition towards CYP2C9. All curcumin derivatives were found to show the total clearance in the range 0.10 log mL/min/kg (compound-**1** and **-4**) to 1.01 log mL/min/kg (compound-**15**). Further, all curcumin derivatives except compound **15** were found to act as OCT2 substrate, thus indicating the potential of these compounds for not having any adverse interactions and no negative effect on renal clearance.

Conclusion and Discussion

The spike proteins of corona viruses are essential for entry of the virus into the target cells. The spike protein exists as a trimer on the surface of the virus with one of the monomer in up conformation and the other two in down conformation (Wrapp et al. 2020). The N-terminal region (S1) of the S protein is important for binding to the cellular receptor ACE2 (Hoffmann et al. 2020; Tai et al. 2020). The S protein undergoes priming by cellular protease, TMPRSS2 and the S2 region of the protein is responsible for fusion of viral and cellular membrane (Hoffmann et al. 2020). Therefore, identifying therapeutics for the S protein of the novel corona virus could potentially target the critical process of entry and fusion of the virus.

Curcumin and its derivatives are known for their many biological activities, one of them is its antiviral activity. Therefore, in this paper, we looked into the potential of curcumin, and its derivatives, to bind to the SARS-CoV and SARS-CoV-2 spike protein. From our computational molecular docking approach (using auto dock 4.2, PDB ID - 6CRV, 6M0J) and in-silico ADMET tool, we predicted that **Bis demethoxy curcumin**, compound-4 and compound-2 were the most recommended curcumin compounds which bind to RBD of the SARS-CoV-2 Spike RBD and SARS-CoV spike protein efficiently in *in silico* studies.

Curcumin has earlier shown to have specific inhibitory effect on the NA activity in influenza virus (Chen et al. 2013; Richart et al. 2018) and modulating immune response to prevent injury

to the lung tissue (Han et al. 2018). Till date, **Bis demethoxy curcumin** has shown to have anti-cancer and hepato-protective activities (Rajagopalan, Sridharana & Menon 2010; Kumaravel, Sankar, Latha, Benson & Rukkumani 2013). This is the first time; it is predicted to have a potential anti-viral activity. Therefore, these curcumin derivatives, which have been predicted to bind to the SARS-CoV-2 spike protein, could be explored as probable inhibitors of COVID-19 spike protein through experimental studies.

Conflicts of Interest

The authors declare that they have no conflict of interests

Acknowledgements

We thank the Dept. of Biochemistry, Indian Academy Degree College - Autonomous, Bengaluru and Ramanbhai Patel College of Pharmacy, Charotar University of Science and Technology, Gujarat for their support in carrying out this work.

References

(2012). Discovery Studio Visualizer Software. Version 3.1. http://www.accelrys.com

Ahmed, S. F., Quadeer, A. A. & McKay, M. R. (2020). Preliminary Identification of Potential Vaccine Targets for the COVID-19 Coronavirus (SARS-CoV-2) Based on SARS-CoV Immunological Studies. *Viruses 12*.

Chen, N., Zhou, M., Dong, X., Qu, J., Gong, F., Han, Y., Qiu, Y., Wang, J., Liu, Y. & Wei, Y. (2020). Epidemiological and clinical characteristics of 99 cases of 2019 novel coronavirus pneumonia in Wuhan, China: a descriptive study. *The Lancet 395*: 507-513.

Chen, T. Y., Chen, D. Y., Wen, H. W., Ou, J. L., Chiou, S. S., Chen, J. M., Wong, M. L. & Hsu, W. L. (2013). Inhibition of enveloped viruses infectivity by curcumin. *PLoS One 8*: e62482.

Chen, Y., Guo, Y., Pan, Y. & Zhao, Z. J. (2020). Structure analysis of the receptor binding of 2019-nCoV. *Biochemical and Biophysical Research Communications 525*: 135-140.

Gorbalenya, A. E. (2020). Severe acute respiratory syndrome-related coronavirus-The species and its viruses, a statement of the Coronavirus Study Group. *BioRxiv*.

Han, S., Xu, J., Guo, X. & Huang, M. (2018). Curcumin ameliorates severe influenza pneumonia via attenuating lung injury and regulating macrophage cytokines production. *Clin Exp Pharmacol Physiol 45*: 84-93.

Hoffmann, M., Kleine-Weber, H., Kruger, N., Muller, M., Drosten, C. & Pohlmann, S. (2020). The novel coronavirus 2019 (2019-nCoV) uses the SARS-coronavirus receptor ACE2 and the cellular protease TMPRSS2 for entry into target cells. *BioRxiv*: 2020.2001.2031.929042.

Huang, C., Wang, Y., Li, X., Ren, L., Zhao, J., Hu, Y., Zhang, L., Fan, G., Xu, J. & Gu, X. (2020). Clinical features of patients infected with 2019 novel coronavirus in Wuhan, China. *The Lancet 395*: 497-506.

Jiang, S., Shi, Z., Shu, Y., Song, J., Gao, G. F., Tan, W. & Guo, D. (2020). A distinct name is needed for the new coronavirus. *The Lancet 395*: 949.

Kahn, J. S. & McIntosh, K. (2005). History and recent advances in coronavirus discovery. *Pediatr Infect Dis J 24*: S223-227, discussion S226.

Khor, P. Y., Aluwi, M. F. F. M., Rullah, K. & Lam, K. W. (2019). Insights on the synthesis of asymmetric curcumin derivatives and their biological activities. *European journal of medicinal chemistry*: 111704.

Kocaadam, B. & Åžanlier, N. (1080). Curcumin, an active component of turmeric (Curcuma longa), and its effects on health. *Crit Rev Food Sci Nutr 57*: 2889-2895.

Kumaravel, M., Sankar, P., Latha, P., Benson, C. S. & Rukkumani, R. (2013). Antiproliferative effects of an analog of curcumin in Hep-2 cells: a comparative study with curcumin. *Nat Prod Commun 8*: 183-186.

Lal, J., Gupta, S. K., Thavaselvam, D. & Agarwal, D. D. (2016). Synthesis and pharmacological activity evaluation of curcumin derivatives. *Chinese Chemical Letters 27*: 1067-1072.

Li, Q., Guan, X., Wu, P., Wang, X., Zhou, L., Tong, Y., Ren, R., Leung, K. S. M., Lau, E. H. Y. & Wong, J. Y. (2020). Early transmission dynamics in Wuhan, China, of novel coronavirus-infected pneumonia. *New England Journal of Medicine*.

Morris, G. M., Huey, R., Lindstrom, W., Sanner, M. F., Belew, R. K., Goodsell, D. S. & Olson, A. J. (2009). AutoDock4 and AutoDockTools4: Automated docking with selective receptor flexibility. *Journal of Computational Chemistry 30*: 2785-2791.

Phelan, A. L., Katz, R. & Gostin, L. O. (2020). The novel coronavirus originating in Wuhan, China: challenges for global health governance. *Jama 323*: 709-710.

Pires, D. E. V., Blundell, T. L. & Ascher, D. B. (2015). pkCSM: Predicting Small-Molecule Pharmacokinetic and Toxicity Properties Using Graph-Based Signatures. *Journal of Medicinal Chemistry 58*: 4066-4072.

Rajagopalan, R., Sridharana, S. & Menon, V. P. (2010). Hepatoprotective role of bis-demethoxy curcumin analog on the expression of matrix metalloproteinase induced by alcohol and polyunsaturated fatty acid in rats. *Toxicol Mech Methods 20*: 252-259.

Richart, S. M., Li, Y. L., Mizushina, Y., Chang, Y. Y., Chung, T. Y., Chen, G. H., Tzen, J. T., Shia, K. S. & Hsu, W. L. (2018). Synergic effect of curcumin and its structural analogue (Monoacetylcurcumin) on anti-influenza virus infection. *J Food Drug Anal 26*: 1015-1023.

Sievers, F., Wilm, A., Dineen, D., Gibson, T. J., Karplus, K., Li, W., Lopez, R., McWilliam, H., Remmert, M., Soding, J., Thompson, J. D. & Higgins, D. G. (2011). Fast, scalable generation of high-quality protein multiple sequence alignments using Clustal Omega. *Mol Syst Biol 7*: 539.

Tai, W., He, L., Zhang, X., Pu, J., Voronin, D., Jiang, S., Zhou, Y. & Du, L. (2020). Characterization of the receptor-binding domain (RBD) of 2019 novel coronavirus: implication for development of RBD protein as a viral attachment inhibitor and vaccine. *Cell Mol Immunol*.

Wang, D., Hu, B., Hu, C., Zhu, F., Liu, X., Zhang, J., Wang, B., Xiang, H., Cheng, Z. & Xiong, Y. (2020). Clinical characteristics of 138 hospitalized patients with 2019 novel coronavirus-infected pneumonia in Wuhan, China. *Jama*.

Who (2020). Coronavirus disease 2019 (COVID-19) situation report-56, WHO.

Wiggers, H. J., Zaioncz, S., Cheleski, J., Mainardes, R. M., Khalil, N. M. & Atta ur, R. (2017). Chapter 7 - Curcumin, a Multitarget Phytochemical: Challenges and Perspectives. *Studies in Natural Products Chemistry*, Elsevier. *53***:** 243-276.

Wrapp, D., Wang, N., Corbett, K. S., Goldsmith, J. A., Hsieh, C.-L., Abiona, O., Graham, B. S. & McLellan, J. S. (2020). Cryo-EM structure of the 2019-nCoV spike in the prefusion conformation. *Science 367*: 1260-1263.

Figure legends

Figure 1. **Comparison of Spike glycoprotein of SARS-CoV-2 and SARS-CoV.** (A) Multiple sequence alignment of Spike glycoprotein of SARS-CoV-2 and SARS-CoV. (amino acid 1-720 of SARS-CoV-2). (B) Percentage identity matrix of Spike glycoprotein of SARS-CoV-2 and SARS-CoV.

Figure 2. The structures of curcumin and its derivatives which displayed high affinity for SARS-CoV-2 and SARS-CoV spike proteins.

Figure 3. **Molecular docking of Bis demethoxy curcumin on SARS-CoV spike protein (6CRV). (A)** 3D structure of Spike Glycoprotein Macromolecule. **(B)** Binding Interaction of Bis demethoxy curcumin with amino acid residues of SARS-CoV Spike glycoprotein (PDB ID-6CRV). **(C)** Superimposed binding mode of Bis demethoxy curcumin with SARS-CoV Spike protein. **(D)** 2D representation of the binding interaction of Bis demethoxy curcumin with SARS-CoV Spike protein.

Figure 4. Molecular docking of Bis demethoxy curcumin on SARS-CoV-2 spike protein receptor binding domain (6M0J). (A) 3D structure of SARS-CoV-2 spike protein RBD bound with ACE2 protein Macromolecule. **(B)** Binding Interaction of Bis demethoxy curcumin with amino acid residue of spike protein RBD of SARS-CoV-2 (PDB ID-6M0J). **(C)** Superimposed binding mode of Bis demethoxy curcumin, docked with SARS-CoV-2 spike protein RBD. **(D)** 2D representation of the binding interaction of Bis demethoxy curcumin with SARS-CoV-2 spike RBD.

Figure 1 (A) CLUSTAL O (1.2.4) multiple sequence alignment

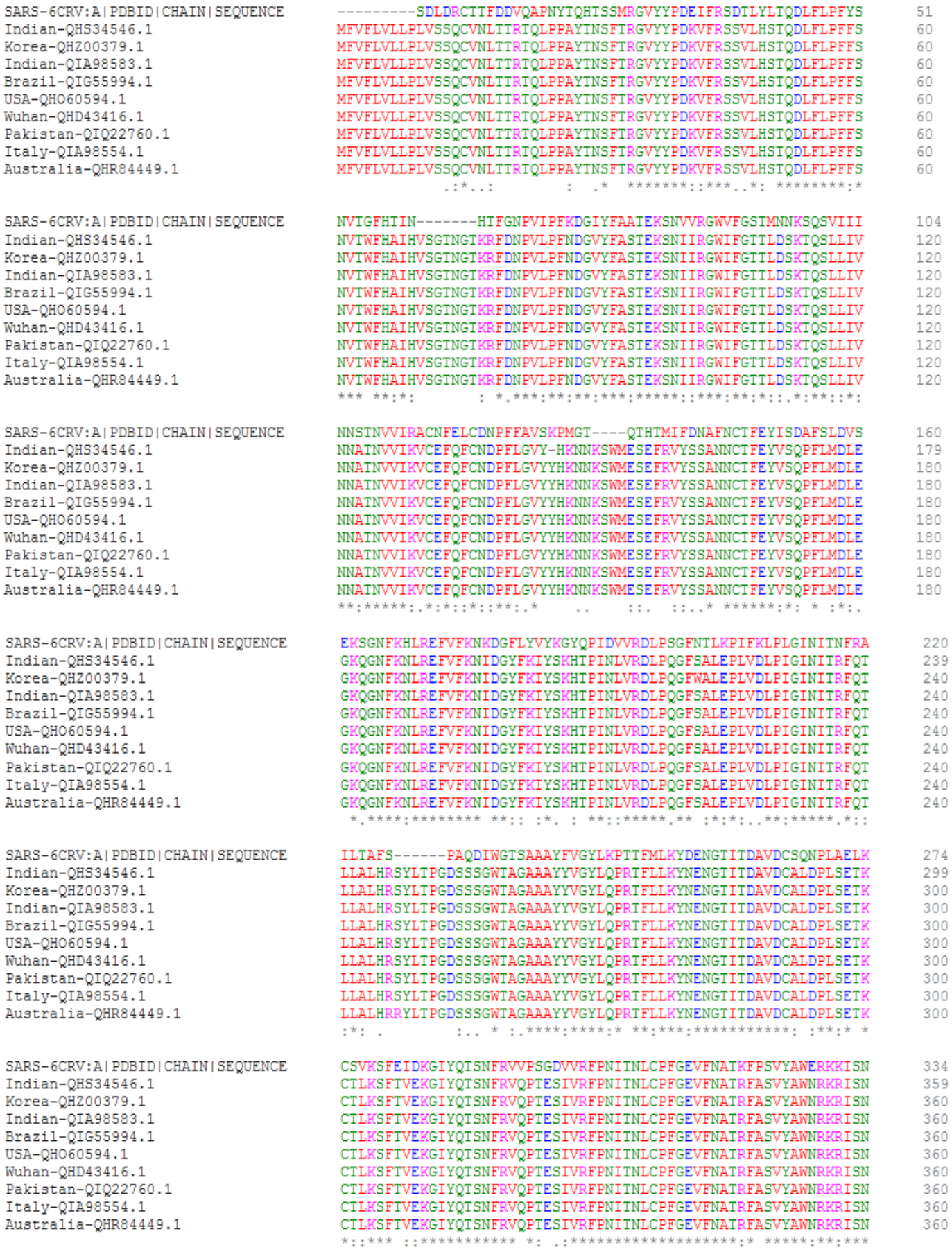

```
SARS-6CRV:A|PDBID|CHAIN|SEQUENCE    CVADYSVLYNSTFFSTFKCYGVSATKLNDLCFSNVYADSFVVKGDDVRQIAPGQTGVIAD  394
Indian-QHS34546.1                   CVADYSVLYNSASFSTFKCYGVSPTKLNDLCFTNVYADSFVIRGDEVIQIAPGQTGKIAD  419
Korea-QHZ00379.1                    CVADYSVLYNSASFSTFKCYGVSPTKLNDLCFTNVYADSFVIRGDEVRQIAPGQTGKIAD  420
Indian-QIA98583.1                   CVADYSVLYNSASFSTFKCYGVSPTKLNDLCFTNVYADSFVIRGDEVRQIAPGQTGKIAD  420
Brazil-QIG55994.1                   CVADYSVLYNSASFSTFKCYGVSPTKLNDLCFTNVYADSFVIRGDEVRQIAPGQTGKIAD  420
USA-QHO60594.1                      CVADYSVLYNSASFSTFKCYGVSPTKLNDLCFTNVYADSFVIRGDEVRQIAPGQTGKIAD  420
Wuhan-QHD43416.1                    CVADYSVLYNSASFSTFKCYGVSPTKLNDLCFTNVYADSFVIRGDEVRQIAPGQTGKIAD  420
Pakistan-QIQ22760.1                 CVADYSVLYNSASFSTFKCYGVSPTKLNDLCFTNVYADSFVIRGDEVRQIAPGQTGKIAD  420
Italy-QIA98554.1                    CVADYSVLYNSASFSTFKCYGVSPTKLNDLCFTNVYADSFVIRGDEVRQIAPGQTGKIAD  420
Australia-QHR84449.1                CVADYSVLYNSASFSTFKCYGVSPTKLNDLCFTNVYADSFVIRGDEVRQIAPGQTGKIAD  420
                                    ***********: ********** ********:********:::**:* ******** ***

SARS-6CRV:A|PDBID|CHAIN|SEQUENCE    YNYKLPDDFMGCVLAWNTRNIDATSTGNYNYKYRYLRHGKLRPFERDISNVPFSPDGKPC  454
Indian-QHS34546.1                   YNYKLPDDFTGCVIAWNSNNLDSKVGGNYNYLYRLFRKSNLKPFERDISTEIYQAGSTPC  479
Korea-QHZ00379.1                    YNYKLPDDFTGCVIAWNSNNLDSKVGGNYNYLYRLFRKSNLKPFERDISTEIYQAGSTPC  480
Indian-QIA98583.1                   YNYKLPDDFTGCVIAWNSNNLDSKVGGNYNYLYRLFRKSNLKPFERDISTEIYQAGSTPC  480
Brazil-QIG55994.1                   YNYKLPDDFTGCVIAWNSNNLDSKVGGNYNYLYRLFRKSNLKPFERDISTEIYQAGSTPC  480
USA-QHO60594.1                      YNYKLPDDFTGCVIAWNSNNLDSKVGGNYNYLYRLFRKSNLKPFERDISTEIYQAGSTPC  480
Wuhan-QHD43416.1                    YNYKLPDDFTGCVIAWNSNNLDSKVGGNYNYLYRLFRKSNLKPFERDISTEIYQAGSTPC  480
Pakistan-QIQ22760.1                 YNYKLPDDFTGCVIAWNSNNLDSKVGGNYNYLYRLFRKSNLKPFERDISTEIYQAGSTPC  480
Italy-QIA98554.1                    YNYKLPDDFTGCVIAWNSNNLDSKVGGNYNYLYRLFRKSNLKPFERDISTEIYQAGSTPC  480
Australia-QHR84449.1                YNYKLPDDFTGCVIAWNSNNLDSKVGGNYNYLYRLFRKSNLKPFERDISTEIYQAGSTPC  480
                                    ********* ***:***:.*:*:.  ***** ** :*:.:*:*******.  :. ...**

SARS-6CRV:A|PDBID|CHAIN|SEQUENCE    TP-PALNCYWPLNDYGFYTTTGIGYQPYRVVVLSFELLNAPATVCGPKLSTDLIKNQCVN  513
Indian-QHS34546.1                   NGVEGFNCYFPLQSYGFQPTNGVGYQPYRVVVLSFELLHAPATVCGPKKSTNLVKNKCVN  539
Korea-QHZ00379.1                    NGVEGFNCYFPLQSYGFQPTNGVGYQPYRVVVLSFELLHAPATVCGPKKSTNLVKNKCVN  540
Indian-QIA98583.1                   NGVEGFNCYFPLQSYGFQPTNGVGYQPYRVVVLSFELLHAPATVCGPKKSTNLVKNKCVN  540
Brazil-QIG55994.1                   NGVEGFNCYFPLQSYGFQPTNGVGYQPYRVVVLSFELLHAPATVCGPKKSTNLVKNKCVN  540
USA-QHO60594.1                      NGVEGFNCYFPLQSYGFQPTNGVGYQPYRVVVLSFELLHAPATVCGPKKSTNLVKNKCVN  540
Wuhan-QHD43416.1                    NGVEGFNCYFPLQSYGFQPTNGVGYQPYRVVVLSFELLHAPATVCGPKKSTNLVKNKCVN  540
Pakistan-QIQ22760.1                 NGVEGFNCYFPLQSYGFQPTNGVGYQPYRVVVLSFELLHAPATVCGPKKSTNLVKNKCVN  540
Italy-QIA98554.1                    NGVEGFNCYFPLQSYGFQPTNGVGYQPYRVVVLSFELLHAPATVCGPKKSTNLVKNKCVN  540
Australia-QHR84449.1                NGVEGFNCYFPLQSYGFQPTNGVGYQPYRVVVLSFELLHAPATVCGPKKSTNLVKNKCVN  540
                                    .   .:***:**:.***  *.*:***************:********* **:*:**:***

SARS-6CRV:A|PDBID|CHAIN|SEQUENCE    FNFNGLTGTGVLTPSSKRFQPFQQFGRDVSDFTDSVRDPKTSEILDISPCAFGGVSVITP  573
Indian-QHS34546.1                   FNFNGLTGTGVLTESNKKFLPFQQFGRDIADTTDAVRDPQTLEILDITPCSFGGVSVITP  599
Korea-QHZ00379.1                    FNFNGLTGTGVLTESNKKFLPFQQFGRDIADTTDAVRDPQTLEILDITPCSFGGVSVITP  600
Indian-QIA98583.1                   FNFNGLTGTGVLTESNKKFLPFQQFGRDIADTTDAVRDPQTLEILDITPCSFGGVSVITP  600
Brazil-QIG55994.1                   FNFNGLTGTGVLTESNKKFLPFQQFGRDIADTTDAVRDPQTLEILDITPCSFGGVSVITP  600
USA-QHO60594.1                      FNFNGLTGTGVLTESNKKFLPFQQFGRDIADTTDAVRDPQTLEILDITPCSFGGVSVITP  600
Wuhan-QHD43416.1                    FNFNGLTGTGVLTESNKKFLPFQQFGRDIADTTDAVRDPQTLEILDITPCSFGGVSVITP  600
Pakistan-QIQ22760.1                 FNFNGLTGTGVLTESNKKFLPFQQFGRDIADTTDAVRDPQTLEILDITPCSFGGVSVITP  600
Italy-QIA98554.1                    FNFNGLTGTGVLTESNKKFLPFQQFGRDIADTTDAVRDPQTLEILDITPCSFGGVSVITP  600
Australia-QHR84449.1                FNFNGLTGTGVLTESNKKFLPFQQFGRDIADTTDAVRDPQTLEILDITPCSFGGVSVITP  600
                                    ************* *.*:* ********:** **:****:* *****:**:*********

SARS-6CRV:A|PDBID|CHAIN|SEQUENCE    GTNASSEVAVLYQDVNCTDVSTAIHADQLTPAWRIYSTGNNVFQTQAGCLIGAEHVDTSY  633
Indian-QHS34546.1                   GTNTSNQVAVLYQDVNCTEVPVAIHADQLTPTWRVYSTGSNVFQTRAGCLIGAEHVNNSY  659
Korea-QHZ00379.1                    GTNTSNQVAVLYQDVNCTEVPVAIHADQLTPTWRVYSTGSNVFQTRAGCLIGAEHVNNSY  660
Indian-QIA98583.1                   GTNTSNQVAVLYQDVNCTEVPVAIHADQLTPTWRVYSTGSNVFQTRAGCLIGAEHVNNSY  660
Brazil-QIG55994.1                   GTNTSNQVAVLYQDVNCTEVPVAIHADQLTPTWRVYSTGSNVFQTRAGCLIGAEHVNNSY  660
USA-QHO60594.1                      GTNTSNQVAVLYQDVNCTEVPVAIHADQLTPTWRVYSTGSNVFQTRAGCLIGAEHVNNSY  660
Wuhan-QHD43416.1                    GTNTSNQVAVLYQDVNCTEVPVAIHADQLTPTWRVYSTGSNVFQTRAGCLIGAEHVNNSY  660
Pakistan-QIQ22760.1                 GTNTSNQVAVLYQDVNCTEVPVAIHADQLTPTWRVYSTGSNVFQTRAGCLIGAEHVNNSY  660
Italy-QIA98554.1                    GTNTSNQVAVLYQDVNCTEVPVAIHADQLTPTWRVYSTGSNVFQTRAGCLIGAEHVNNSY  660
Australia-QHR84449.1                GTNTSNQVAVLYQDVNCTEVPVAIHADQLTPTWRVYSTGSNVFQTRAGCLIGAEHVNNSY  660
                                    ***:*.:***********:* .*********:**:****.*****:**********:.**

SARS-6CRV:A|PDBID|CHAIN|SEQUENCE    ECDIPIGAGICASYHTVSL----LRSTSQKSIVAYTMSLGADSSIAYSNNTIAIPTNFSI  689
Indian-QHS34546.1                   ECDIPIGAGICASYQTQTNSPRRARSVASQSIIAYTMSLGAENSVAYSNNSIAIPTNFTI  719
Korea-QHZ00379.1                    ECDIPIGAGICASYQTQTNSPRRARSVASQSIIAYTMSLGAENSVAYSNNSIAIPTNFTI  720
Indian-QIA98583.1                   ECDIPIGAGICASYQTQTNSPRRARSVASQSIIAYTMSLGAENSVAYSNNSIAIPTNFTI  720
Brazil-QIG55994.1                   ECDIPIGAGICASYQTQTNSPRRARSVASQSIIAYTMSLGAENSVAYSNNSIAIPTNFTI  720
USA-QHO60594.1                      ECDIPIGAGICASYQTQTNSPRRARSVASQSIIAYTMSLGAENSVAYSNNSIAIPTNFTI  720
Wuhan-QHD43416.1                    ECDIPIGAGICASYQTQTNSPRRARSVASQSIIAYTMSLGAENSVAYSNNSIAIPTNFTI  720
Pakistan-QIQ22760.1                 ECDIPIGAGICASYQTQTNSPRRARSVASQSIIAYTMSLGAENSVAYSNNSIAIPTNFTI  720
Italy-QIA98554.1                    ECDIPIGAGICASYQTQTNSPRRARSVASQSIIAYTMSLGAENSVAYSNNSIAIPTNFTI  720
Australia-QHR84449.1                ECDIPIGAGICASYQTQTNSPRRARSVASQSIIAYTMSLGAENSVAYSNNSIAIPTNFTI  720
                                    **************:* :      **.:.:**:********:.*:*****:*******:*
```

Figure 1 (B). Percentage identity Matrix

	SARS	Indian1	Korea	Indian2	Brazil	USA	Wuhan	Pakistan	Italy	Australia
SARS-6CRV	100	73.75	73.77	73.69	73.77	73.77	73.77	73.77	73.77	73.77
Indian1	73.75	100	99.84	99.84	99.92	99.92	99.92	99.92	99.92	99.84
Korea	73.77	99.84	100	99.84	99.92	99.92	99.92	99.92	99.92	99.84
Indian2	73.69	99.84	99.84	100	99.92	99.92	99.92	99.92	99.92	99.84
Brazil	73.77	99.92	99.92	99.92	100	100	100	100	100	99.92
USA	73.77	99.92	99.92	99.92	100	100	100	100	100	99.92
Wuhan	73.77	99.92	99.92	99.92	100	100	100	100	100	99.92
Pakistan	73.77	99.92	99.92	99.92	100	100	100	100	100	99.92
Italy	73.77	99.92	99.92	99.92	100	100	100	100	100	99.92
Australia	73.77	99.84	99.84	99.84	99.92	99.92	99.92	99.92	99.92	100

Figure 1. **Comparison of Spike glycoprotein of SARS-CoV-2 and SARS-CoV.** (A) Multiple sequence alignment of Spike glycoprotein of SARS-CoV-2 and SARS-CoV. (amino acid 1-720 of SARS-CoV-2). (B) Percentage identity matrix of Spike glycoprotein of SARS-CoV-2 and SARS-CoV.

Figure 2

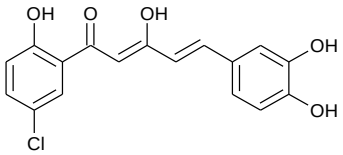

Curc-driav-2

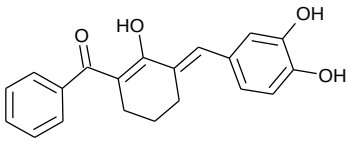

Curc-driav-4

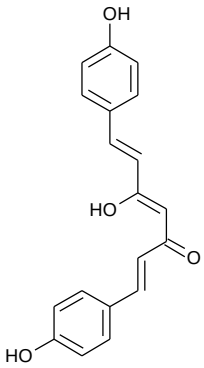

Bis-demethoxy curcumin

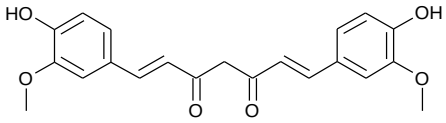

Curcumin

Figure 2. The curcumin and its derivatives which displayed high affinity for SARS-CoV-2 and SARS-CoV spike proteins.

Figure 3

(A)

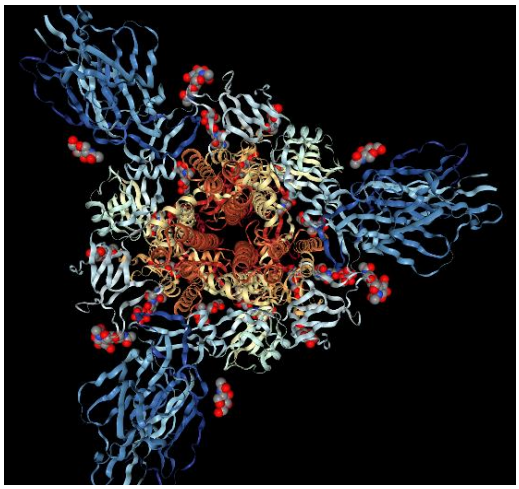

(B)

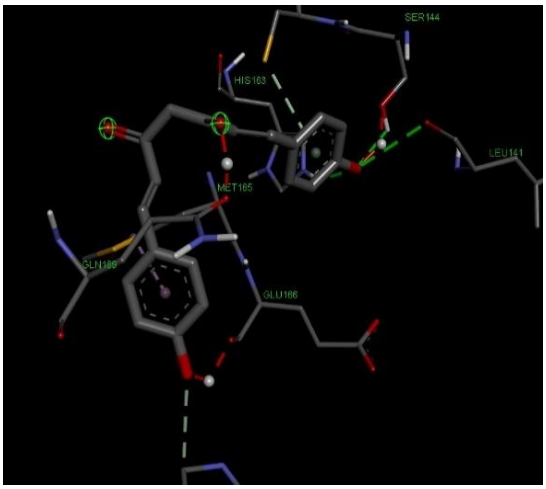

(C)

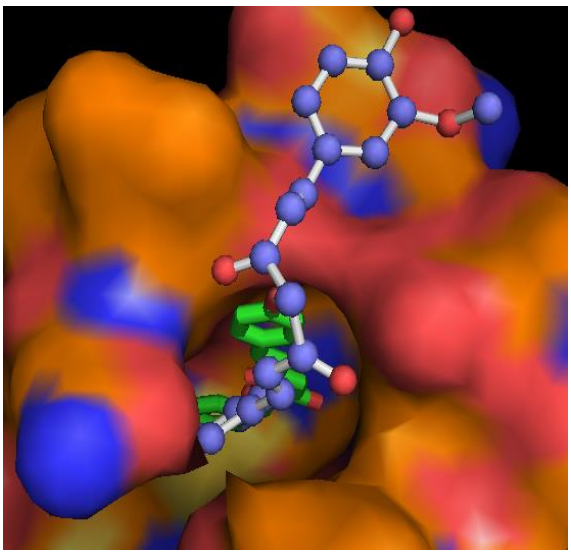

(D)

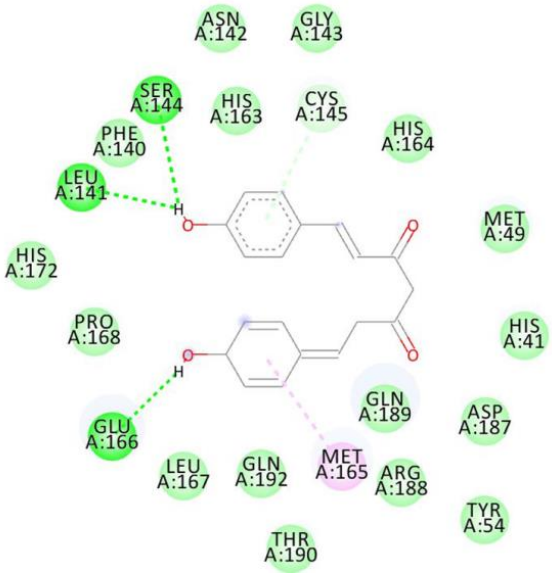

Figure 3. **Molecular docking of Bis demethoxy curcumin on SARS-CoV spike protein (6CRV). (A)** 3D structure of Spike Glycoprotein Macromolecule. **(B)** Binding Interaction of Bis demethoxy curcumin with amino acid residues of SARS-CoV Spike glycoprotein (PDB ID-6CRV). **(C)** Superimposed binding mode of Bis demethoxy curcumin with SARS-CoV Spike protein. **(D)** 2D representation of the binding interaction of Bis demethoxy curcumin with SARS-CoV Spike protein.

Figure 4

(A)

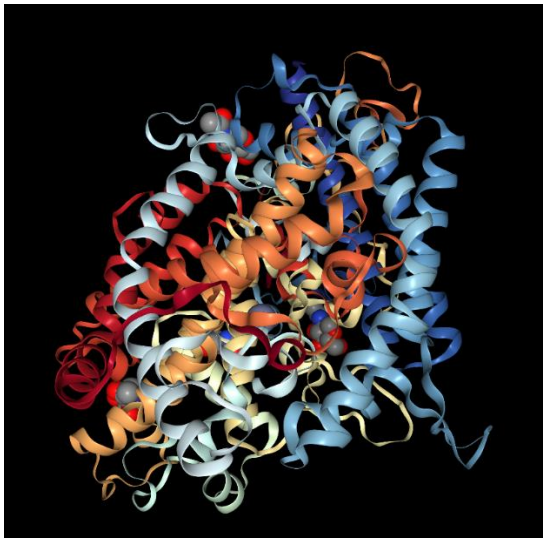

(B)

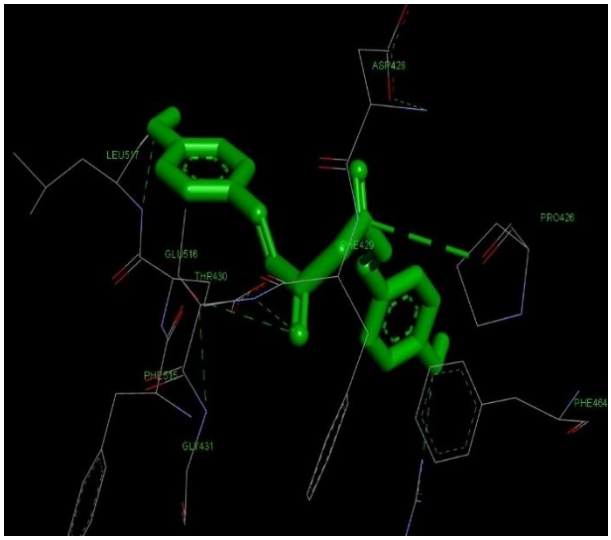

(C)

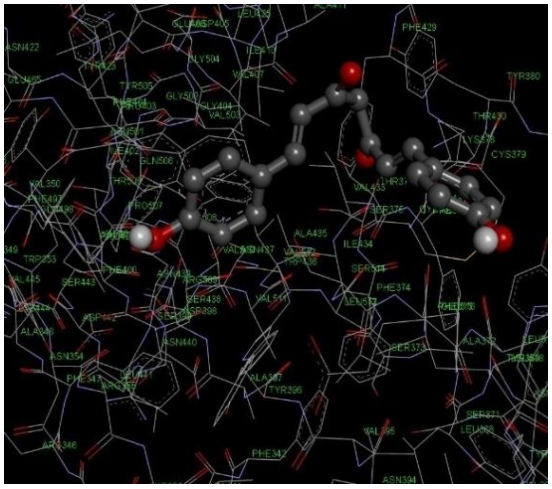

(D)

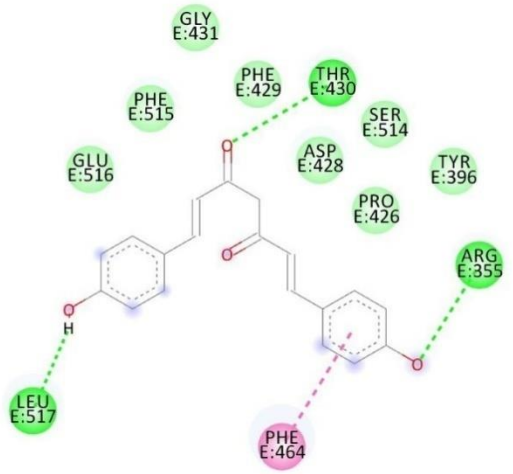

Figure 4. Molecular docking of Bis demethoxy curcumin on SARS-CoV-2 spike protein receptor binding domain (6M0J). (A) 3D structure of SARS-CoV-2 spike protein RBD bound with ACE2 protein Macromolecule. **(B)** Binding Interaction of Bis demethoxy curcumin with amino acid residue of spike protein RBD of SARS-CoV-2 (PDB ID-6M0J). **(C)** Superimposed binding mode of Bis demethoxy curcumin, docked with SARS-CoV-2 spike protein RBD. **(D)** 2D representation of the binding interaction of Bis demethoxy curcumin with SARS-CoV-2 spike RBD.

Table 1: Molecular docking results of curcumin and its derivatives with SARS-CoV Spike protein (6CRV).

Compound	Binding Energy (ΔG)	Ligand Efficiency	Intermolecular energy	XP H-Bond
Curcumin	**-10.2**	**-0.11**	**-8.35**	**-11.6712**
BHBC	-8.01	-0.12	-7.66	-3.48285
MNC	-7.96	-0.34	-7.14	8.29214
BDMC	**-14.18**	**-0.11**	**-12.38**	**-18.0876**
1	-4.04	-0.23	-4.04	0
2	**-8.35**	**-0.41**	**-6.19**	**-21.5297**
3	-6.90	-0.24	-5.62	-12.7728
4	**-8.95**	**-0.17**	**-6.87**	**-20.8219**
5	-7.17	-0.21	-6.33	-8.36051
6	-7.25	-0.41	-6.30	-9.50531
7	-8.09	-0.25	-7.22	-8.46448
8	-7.43	-0.14	-6.74	-6.95328
9	-6.38	-0.16	-6.38	0
10	-7.65	-0.25	-6.84	-8.61098
11	-7.32	-0.21	-5.39	-19.3227
12	-7.62	-0.34	-7.57	-0.472777
13	-6.78	-0.41	-5.42	-13.5985
14	**-8.69**	**-0.28**	**-6.49**	**-22.0052**
15	-7.40	-0.42	-7.36	-0.473228
16	**-8.30**	**-0.21**	**-7.48**	**-8.26615**

DMC	-7.63	-0.15	-8.01	-9.77056
FAC	-7.87	-0.41	-6.65	-10.005
IBC	-7.83	-0.19	-6.87	-7.00
IVC	-7.69	-0.41	-7.13	-21.867
SYC	-7.15	-0.38	-6.13	-10.1353

Abbreviations: BHBC: 3-5-di-tert-butyl-4-hydroxybenzaldehyde curcumin, MNC: 4-methoxy-1-naphthaldehyde curcumin, BDMC: Bisdemethoxy curcumin, DMC: Demethoxy curcumin, FAC: Ferulic-acid curcumin, IBC: Ibuprofen curcumin, IVC: Isovanillin curcumin, SYC: Syringaldehyde curcumin

Table 2: Molecular docking analysis of curcumin and its derivatives with SARS-CoV-2 Spike protein Receptor binding domain (6M0J).

Compound	**Binding Energy (ΔG)**	**Ligand Efficiency**	**Intermolecular energy**	**XP H-Bond**
Curcumin	**-9.81**	**-0.15**	**-8.35**	**-15.1512**
BHBC	-5.33	-0.13	-7.96	0
MNC	-7.96	-0.27	-7.38	-4.24687
BDMC	**-10.01**	**-0.12**	**-9.18**	**-13.9824**
1	-7.58	-0.36	-6.19	-18.3489
2	**-8.81**	**-0.31**	**-8.38**	**1.2654**
3	-6.14	-0.34	-5.45	-6.95102
4	**-8.88**	**-0.18**	**-7.98**	**-14.0321**
5	-6.23	-0.26	-5.88	-3.5891
6	-7.16	-0.37	-6.15	-10.1688
7	-6.89	-0.25	-5.98	-9.12515

8	-5.49	-0.12	-3.90	-5.92265
9	-6.92	-0.18	-6.22	-6.96719
10	-7.03	-0.24	-6.33	-7.0
11	-6.88	-0.27	-6.23	-6.44363
12	-7.95	-0.41	-5.70	-2.5581
13	-6.11	-0.39	-5.42	-7.34943
14	-7.45	-0.19	-6.40	-10.5367
15	-5.74	-0.39	-5.51	-2.36748
16	-7.83	-0.27	-7.48	-6.64321
DMC	-5.98	-0.19	-5.38	-5.99913
FAC	-5.85	-0.38	-5.25	-6.46613
IBC	-6.65	-0.15	-6.20	-1.52841
IVC	**-8.96**	**-0.43**	**-7.73**	**-12.2707**
SYC	-5.87	-0.29	-5.43	-4.4411

Abbreviations: BHBC: 3-5-di-tert-butyl-4-hydroxybenzaldehyde curcumin, MNC: 4-methoxy-1-naphthaldehyde curcumin, BDMC: Bisdemethoxy curcumin, DMC: Demethoxy curcumin, FAC: Ferulic-acid curcumin, IBC: Ibuprofen curcumin, IVC: Isovanillin curcumin, SYC: Syringaldehyde curcumin

Table 3: *In-silico* prediction of drug-likeness for curcumin derivatives [a]

Compound	**MW**	**LogP**	**SA**	**HBA**	**HBD**	**$n_{violations}$**	**Rotatable bonds**
BHBC	534.78	8.93	236.0	4	3	1	6
MNC	538.59	6.14	232.11	7	2	1	11

BDMC	308.33	3.83	133.51	4	3		5
1	270.353	4.21	115.89	3	1		4
2	332.739	3.79	136.57	5	4		4
3	314.337	3.77	133.64	5	4		4
4	322.36	4.36	139.56	3	3		4
5	364.441	4.93	159.62	4	0		5
6	320.388	4.95	141.45	4	3		1
7	325.32	3.60	138.02	5	1		6
8	329.193	4.45	125.75	2	1		4
9	462.181	5.24	164.71	7	2		0
10	351.358	4.13	149.74	4	5		1
11	360.375	5.07	149.89	2	1		3
12	419.565	6.24	185.40	9	4		1
13	389.495	5.22	171.67	4	4		1
14	342.778	3.81	143.82	4	2		2
15	469.629	4.38	208.20	6	5		1
16	486.564	6.19	211.58	11	6	1	0
DMC	342.391	3.20	146.43	5	2		9
FAC	550.604	4.7	232.81	9	2		15
IBC	556.655	5.24	240.62	7	1		15
IVC	504.535	4.69	214.22	8	3		11
SYC	430.453	3.77	180.12	10	8	1	3

[a] MW = Molecular weight, LogP = octanol-water partition coefficient, SA = Surface Area, HBA = Number of hydrogen bond acceptor, HBD = Number of

hydrogen bond donor, nviolations = violations from Lipinski's rule. BHBC: 3-5-di-tert-butyl-4-hydroxybenzaldehyde curcumin, MNC: 4-methoxy-1-naphthaldehyde curcumin, BDMC: Bisdemethoxy curcumin, DMC: Demethoxy curcumin, FAC: Ferulic-acid curcumin, IBC: Ibuprofen curcumin, IVC: Isovanillin curcumin, SYC: Syringaldehyde curcumin

Table 4: *In-silico* ADME prediction for curcumin derivatives[a]

Comp	Absorption						Distribution				Metabolism		Excretion	
	WS	**CP**	**IA**	**SP**	**PI-1**	**PI-2**	**VD**	**FU**	**BBB**	**CNS**	**CI-1**	**CI-2**	**TC**	**RS**
BHBC	-2.91	0.67	88.62	-2.73	Yes	Yes	-0.39	0.31	-0.67	-0.85	No	Yes	0.15	No
MNC	-3.64	0.43	100	-2.73	Yes	Yes	-1.45	0.33	-0.39	-2.73	Yes	Yes	0.26	No
BDMC	-4.43	1.01	95.92	-2.99	No	No	-0.22	0.08	-0.72	-2.11	Yes	Yes	0.12	No
1	-4.66	1.25	91.80	-2.51	No	No	0.18	0.06	0.01	-1.45	Yes	Yes	0.10	No
2	-3.23	0.93	89.16	-2.76	No	No	-0.07	0.12	-1.07	-2.29	Yes	Yes	0.05	No
3	-3.19	0.94	89.70	-2.76	No	No	-0.02	0.13	-1.06	-2.27	Yes	Yes	0.06	No
4	-4.11	0.92	87.64	-3.07	No	No	0.09	0	-0.74	-1.85	Yes	Yes	0.10	No
5	-6.39	1.06	94.85	-2.49	No	No	0.25	0	-0.03	-1.30	Yes	Yes	0.22	No
6	-5.42	1.43	90.49	-2.73	No	No	0.05	0	-0.33	-1.29	Yes	Yes	0.23	No
7	-4.54	1.04	91.97	-2.73	No	No	-0.37	0	0.28	-2.20	Yes	Yes	0.13	No
8	-5.09	1.66	90.44	-2.29	No	No	0.27	0	0.16	-1.47	No	Yes	0.14	No
9	-7.03	1.13	93.34	-2.51	No	No	0.37	0	0.46	-1.26	Yes	Yes	0.26	No
10	-4.89	0.94	91.50	-2.74	No	No	-0.04	0	-0.24	-1.93	Yes	Yes	0.11	No
11	-5.93	1.28	89.16	-2.59	No	No	0.36	0	0.66	-1.40	No	Yes	0.13	No
12	-6.99	1.02	91.30	-2.75	No	No	0.66	0	-0.32	-1.85	Yes	Yes	1.04	No
13	-5.42	1.27	92.76	-2.80	Yes	Yes	0.54	0	-0.02	-1.58	Yes	Yes	0.26	No

14	-4.20	1.12	90.31	-2.92	No	No	-0.04	0.01	-0.31	-1.33	No	Yes	0.08	No
15	-3.76	0.97	88.86	-2.79	No	No	1.90	0.16	-0.20	-1.26	No	No	1.01	Yes
16	-6.92	0.90	94.67	-2.73	No	No	-0.59	0.07	-0.72	-2.62	No	Yes	0.41	No
DMC	-3.95	0.99	92.03	-2.74	No	No	-0.06	0.12	-0.23	-2.66	Yes	Yes	0.32	No
FAC	-4.02	1.41	83.68	-2.76	Yes	Yes	-0.58	0.24	-0.91	-3.26	Yes	Yes	0.55	No
IBC	-4.36	0.91	91.72	-2.73	No	No	-0.88	0.18	-0.53	-2.77	Yes	Yes	0.62	No
IVC	-3.95	0.96	89.31	-2.73	No	No	-0.60	0.24	-1.37	-3.02	Yes	Yes	0.16	No
SYC	-3.89	1.01	89.15	-2.73	No	No	0.28	0.17	-1.47	-3.14	Yes	Yes	0.23	No

[a] Abbreviations: WS – Water solubility (log mol/L), CP – Caco2 permeability (log Papp in 10-6 cm/s), IA – Human intestinal absorption (% Absorbed), SP – Skin permeability (log Kp), PI-1 – P-glycoprotein I inhibitor, PI-2 – P-glycoprotein II inhibitor, VD – Human volume of distribution (log L/kg), FU – Fraction unbound (human) (Fu), BBB – BBB permeability (logBB), CNS – CNS permeability (log PS), CI-1 – CYP3A4 inhibitor, CI-2 – CYP2C9 inhibitor, TC – Total clearance (log mL/min/kg), RS – Renal OCT2 (organic cation transporter 2) substrate. BHBC-3-5-di-tert-butyl-4-hydroxybenzaldehyde curcumin, MNC-4-methoxy-1-naphthaldehyde curcumin, BDMC-Bisdemethoxy curcumin, DMC-Demethoxy curcumin, FAC-Ferulic-acid curcumin, IBC-Ibuprofen curcumin, IVC-Isovanillin curcumin, SYC-Syringaldehyde curcumin

Supplementary Figure 1: The curcumin and its derivatives which were used for the docking studies.

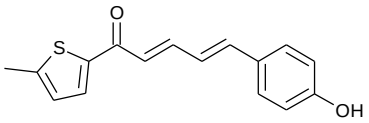

Curc-deriv-1

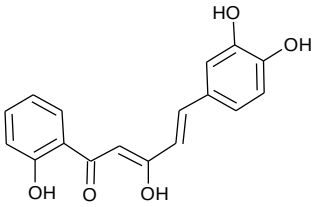

Curc-deriv-3

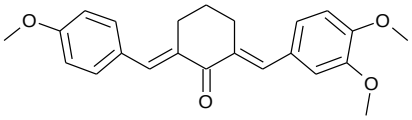

Curc-deriv-5

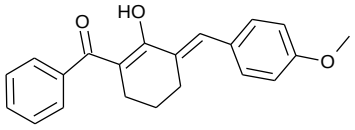

Curc-deriv-6

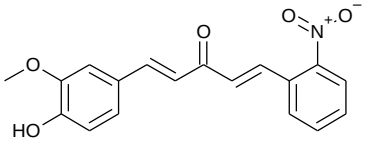

Curc-deriv-7

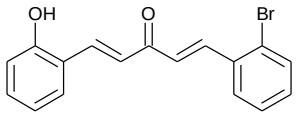

Curc-deriv-8

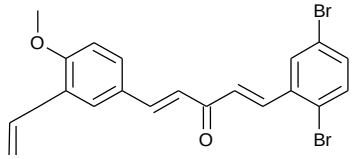

Curc-deriav-9

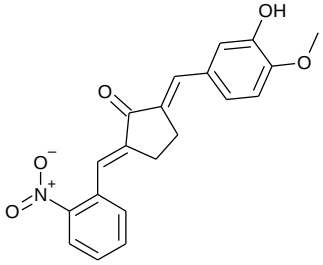

Curc-deriv-10

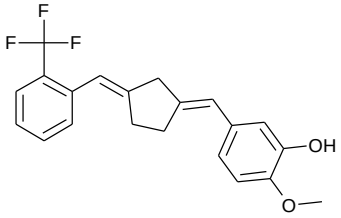

Curc-deriv-11

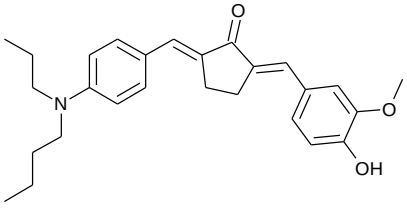

Curc-deriv-12

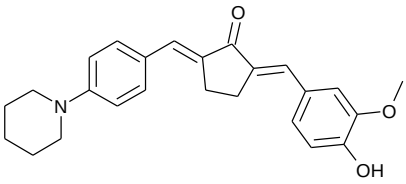

Curc-deriv-13

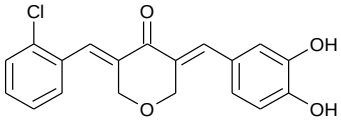

Curc-deriv-14

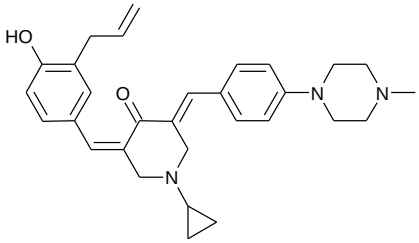

Curc-deriv-15

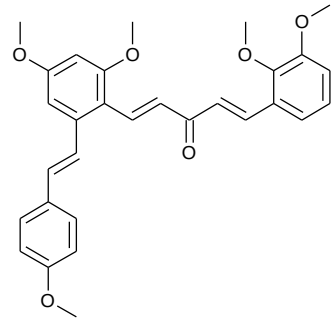

Curc-deriv-16

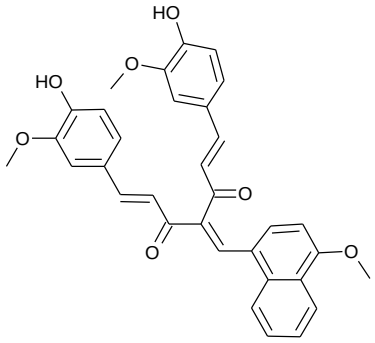

4-methoxy-1-naphthaldehyde curcumin (MNC)

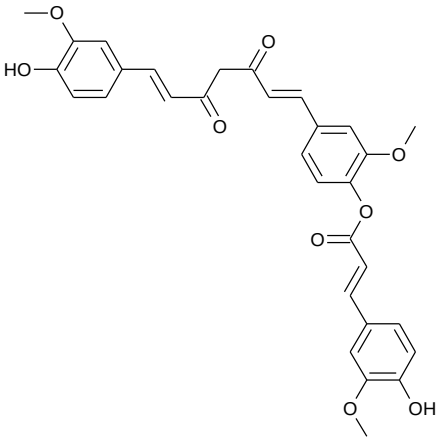

Ibuprofen curcumin (IBC)

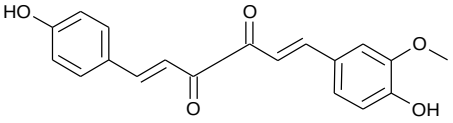

Demethoxy curcumin (DMC)

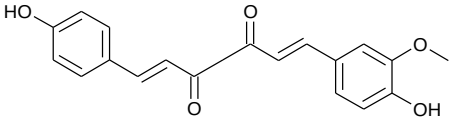

Ferulic-acid curcumin (FAC)

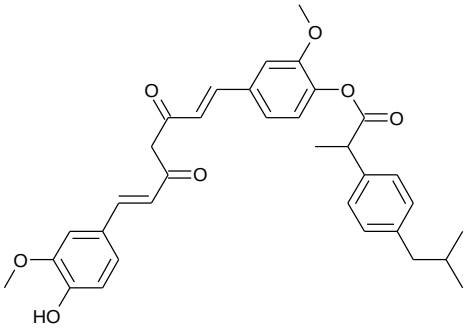

Isovanillin curcumin (IVC)

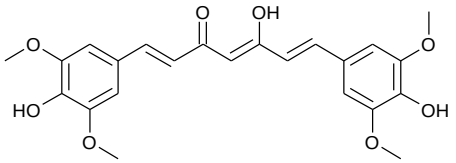

Syringaldehyde curcumin (SYC)

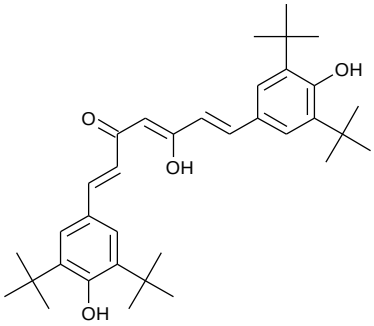

3-5-di-tert-butyl-4-hydroxybenzaldehyde curcumin (BHBC)